

Numerical Analysis of Lamb Wave Propagation in Composite Plate With Different Fiber Orientation Angles – Acoustic Emission Approach

Jakub Rzeczkowski¹

¹ Faculty of Mathematics and Information Technology, Lublin University of Technology, Nadbystrzycka 38, 20-618 Lublin, Poland

E-mail: j.rzeczkowski@pollub.pl

ABSTRACT

This paper aims at numerical finite element (FEM) research of guided Lamb waves propagation in multidirectional composite plates. All simulations were conducted in the Abaqus/CAE software by using the dynamic/explicit solver. The material considered in this work was carbon/epoxy composite laminate with $[90^\circ/\theta/\theta/\theta/-\theta/-\theta/90^\circ]$ stacking sequence where θ set was equal 0° , 30° , 45° , 60° and 90° . The main goal of the analysis was to evaluate the influence of fiber orientation angles θ on propagation behavior of the separate symmetric S_0 and asymmetric A_0 Lamb wave modes. Numerical model was created by using the C3D8R brick element. The Lamb waves were generated by using concentrated force with 200 kHz frequency. The acoustic signal generated by travelling wave was registered at two nodes that represent the acoustic emission sensors. Obtained results were presented in tabular form where separate mode velocities were collected and on the normalized displacement versus time plots depicted registered wave signals. In addition, the contour diagrams and through-thickness deformations plots were created to present behavior of the extensional and the flexural modes. The greatest value of the S_0 mode velocity was obtained for unidirectional laminates whereas the lowest for composite plate with 45° fiber orientation angle. The asymmetric mode found to generate slightly greater deformation of plate in XZ plane than the symmetric. Recognition of the Lamb wave behavior in multidirectional laminates will allow to better planning the experimental acoustic emission tests.

Keywords: acoustic emission, Lamb wave, numerical analysis, composite laminates.

INTRODUCTION

Acoustic emission (AE) is one of the techniques belonging to the group of the structural health monitoring (SHM) methods [1]. The measurements of AE signals are conducted in order to localization and classification of elastic wave sources generate by surface and internal failure occurred in different structures. This technique is finding employment in various industry branches where non-destructive diagnosis of load-bearing components is demand, for example in aircraft structures or in testing the pressure vessels. In recent years, applicability of the acoustic emission technique has been extended to composite laminates research fields. Thanks to high sensitivity, this method can easily detect different microscale defects occur in the form of cracks or structural

flaw. Referring to the fiber reinforced composites, the AE technique [2–6] is a promising tool in detection of delamination phenomenon [7–9] that is the most common type of failure in that type of materials. The basic principle of the AE method is detection of elastic waves generated by strain energy accumulated inside material and released during development of fracture mechanism. The acoustic signals are often register by using the piezoelectric sensors. Moreover, the AE mechanisms generate high-frequency signals with low amplitude, so it is not recognize by human ears. The basic definition of elastic wave phenomenon is a particle motion in specified directions. Thus, the acoustic emission signal can consist of different type of waves as transverse, longitudinal or other. For the first case, the particles move in perpendicular direction to the propagating wave,

whereas for the latter, the particles vibrate along this direction. Considering real structures, the damage mechanism sources can generate complex acoustic signal that consists of both, the longitudinal and shear waves, commonly called “body waves”. Therefore, in order to study application of the acoustic emission technique in detecting of damage phenomena in different structures, the examination of Lamb waves [6,10], that consisted of superposition of various modes, indicate to be the most appropriate approach. The aforementioned Lamb waves are present in thin plates and they are dependent on structural geometry, entry angle or excited load. They are represented by the symmetric S_0 and asymmetric A_0 modes simultaneously, that can be described by the Equations 1 and 2.

$$\frac{\tanh\left(\frac{\beta d}{2}\right)}{\tanh\left(\frac{\alpha d}{2}\right)} = \frac{4\alpha\beta k^2}{(k^2 + \beta^2)^2} \quad (1)$$

$$\frac{\tanh\left(\frac{\beta d}{2}\right)}{\tanh\left(\frac{\alpha d}{2}\right)} = \frac{(k^2 + \beta^2)^2}{4\alpha\beta k^2} \quad (2)$$

where: d – a plate thickness,
 k – wavenumber,
 α and β – calculation coefficients dependent on extensional, transverse and phase velocities respectively [14].

The main advantage of the Lamb wave is possibility to propagate on large distance in materials with significant attenuation ratio, such as carbon/epoxy. On the other hand, it is susceptible to interfere with damage or boundary conditions [16]. Therefore, in the point of view of the acoustic emission testing, there is a continuous need to better recognition of elastic wave propagation behavior. The knowledge about damage mechanism source, its characteristic properties and influence on generated elastic wave has a crucial meaning in proper planning and conducting of the AE testing. Taking into account this features, many researchers analyzed experimentally [18–21] and numerically [11–13] the issues of Lamb wave propagation in composite structures. For example, in [15] Cheng et. al. conducted experimental and numerical study of real I-shaped girder. They utilized effective method of damage source localization that based on application of the artificial neural network. Obtained outcomes were compared with numerical FE simulations based on the Lamb wave propagations. Another authors [17]

prepared numerical investigation of Lamb wave interaction with different parameters of implemented defect. Elaborated conclusions proved considerable influence of defect orientation on wave propagation. In [22] presented numerical analysis on influence of different geometrical properties of metallic foam sandwich panels on Lamb waves propagation. It was concluded that this process was dependent on such parameters as: relative density, grain size or geometrical dimensions. To sum up, as it was evidenced in many papers, the Lamb wave is influenced by the type of medium that it travels inside. Therefore, elastic wave propagation behavior in composite structures have to be deeply understand when the AE testing is utilize to zonal defect localization.

In this paper presented numerical finite element simulations of Lamb wave propagation in thin composite plate. All simulations were conducted in Abaqus/CAE by using dynamic/explicit solver. The novelty in current work is evaluation of influence of different fiber orientation angles on guided Lamb waves propagation. Knowledge about the behavior of symmetric and asymmetric modes generated by the damage allow to better plan the experimental acoustic emission measurements.

NUMERICAL ANALYSIS

Numerical analysis of Lamb wave propagation in multidirectional composite laminates were conducted in the Abaqus/CAE finite element software by using the dynamic explicit calculation solver. All simulations were prepared on the Lenovo ThinkPad T14s workstation with eight core processors 11th Gen Intel(R) (TM) i5-1145G7 2.6 GHz. Additionally, in order to reduce computational time a parallelization option was used. The composite model was created as a solid square plate with the main dimensions of 200 mm x 200 mm and total thickness of 1.048 mm. Subsequently, the plate model was divided into eight plies representing individual layers of multidirectional carbon fiber reinforced composite laminates – all those layers had a thickness of 0.131 mm. The engineering constant values and mass density assigned to composite plate were obtained during preliminary tensile tests and were collected in the Table 1. During all simulations considered laminates with $[90^\circ/\theta/\theta/\theta/-\theta/-\theta/-\theta/90^\circ]$ symmetric stacking sequence with θ set equal 0° ,

Table 1. Materials properties of the carbon/epoxy laminate

E_{11} [MPa]	E_{22} [MPa]	E_{33} [MPa]	ν_{12} [-]	ν_{13} [-]	ν_{23} [-]	G_{12} [MPa]	G_{13} [MPa]	G_{23} [MPa]	ρ [km/m ³]
112105	7421	7421	0.27	0.27	0.34	3338	3338	2769	1668

30°, 45°, 60° and 90°. The symmetric configuration was chosen due to zero B_{16} and D_{16} terms in elastic couplings matrix, thus the effects of elastic couplings phenomena were limited.

In order to get accurate results of wave propagation during finite element analysis two appropriate conditions must be fulfilled, namely: time increment size and element size. Those parameters are highly dependent on the type of wave that is being predicted to capture. Thus, the time increment size (δt) should be selected in that way to allow capture the smallest natural period of interest. In other words, during each time step the distance that Lamb wave travels is required to be smaller than the distance between two adjacent elements. The values of δt can be estimated by using the Courant-Friedrichs-Lewy (CFL) condition described by the Equation 3, where f_{max} is the frequency applied during FE simulation to Lamb wave excitation. For all numerical analysis the f_{max} was chosen as 200 kHz. Based on the CFL criterion the value of δt was established as 2.5×10^{-7} s and $\delta t = 1 \times 10^{-7}$ s was selected as being sufficient to capture Lamb wave travelled in multidirectional composite plate.

$$\delta t < \frac{1}{20 * f_{max}} \tag{3}$$

For the latter condition, the Blakes criterion (Equation 4) describes the maximum element size (L_{max}). Here, the n_{min} is the number of finite elements per Lamb wavelength (selected as $n = 10$ for all simulations) and C is a theoretical elastic propagation speed.

$$L_{max} < \frac{C}{f_{max} * n_{min}} \tag{4}$$

According to the recommendation concerning L_{max} that comes from above criterion, the whole model was divided into 320000 linear hexahedral C3D8R reduced integration 3D element with dimensions of 1 mm in x and y directions. In order to numerical evaluation of influence of fiber orientation angle on Lamb wave propagation in composite materials, three specific nodes were selected; one as an actuator and two as an acoustic emission sensors. The laminate

plate geometry with specified nodes was given in Figure 1. The load excitation signal was applied to the node at the distance of 10 mm from the YZ principal plane. Subsequently, the second and third nodes away 140 mm and 190 mm from YZ plane were employed as the acoustic emission sensors AE1 and AE2 respectively. During finite element simulations, the AE sensors registered normalized amplitude of Lamb wave represented in time domain. Additionally, the A_0 and S_0 modes of propagated elastic waves were generated separately. This possibility of numerical simulations is a big advantage over experimental tests that are not allowed to distinguished between different propagation modes. In current model, the A_0 mode was applied by generating the load only on the top surface of composite plate model (load configuration 1, LC-1), whereas the S_0 mode was excited by application of frequency load to the bottom and top composite surfaces simultaneously (load configuration 2, LC-2). This procedure is beneficial in the point of view of understanding the propagational behavior of separate Lamb wave modes in composite structures. To calculate the A_0 and S_0 modes velocities a simply relation

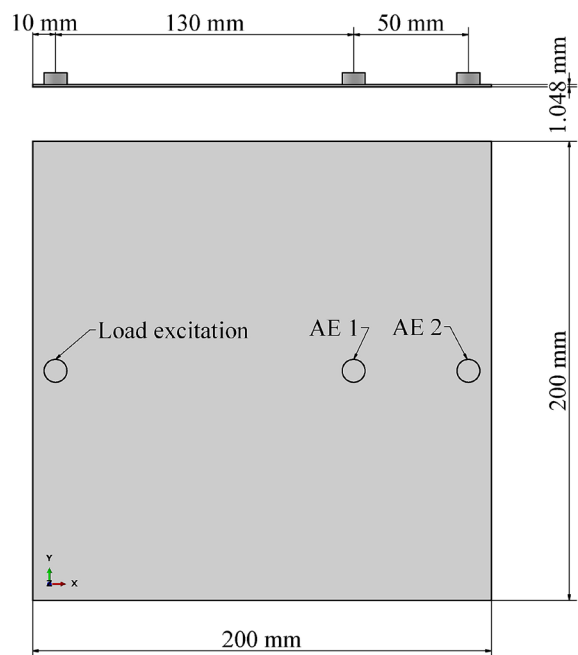


Fig. 1. Geometrical dimensions of the composite plate numerical model

presented in the Equation 5 was used, where ΔX is the distance between AE1 and AE2 sensors ($\Delta X = 50$ mm) and ΔT is a difference between arrival time to subsequent receivers.

$$V = \frac{\Delta X}{\Delta T} \quad (5)$$

RESULTS AND DISCUSSION

In Figures 2, 3, 4, 5 and 6 shown acoustic emission signals of Lamb waves registered by the AE1 and AE2 numerical sensors presented in the form of the normalized displacement versus time plots obtained for two different cases of excited signal. According to the AE data analysis two different approaches can be used to assess recorded acoustic emission signal, namely: the parameter-based and the waveform-based analysis. In case of the first approach, the acoustic wave can be described by basic signal parameters such as: peak amplitude (RMS), rise time, duration or energy. On the other hand, for the latter approach, the AE signals is processed by using different techniques, for example by application of the frequency analysis. Considering all composite plate models with unidirectional and multidirectional configurations two different stages can be observed. Regarding to the first stage, for time period from 0 μ s up to around 40 μ s, registered signals characterized continuous emission. This was an evidence on extensional Lamb wave mode propagation. For the latter, the captured signals transformed to the transient emission that is characteristic for flexural asymmetric mode. The S_0 mode reached the

greatest peak amplitude only for unidirectional composite plate. For multidirectional layer configurations the anisotropy of material strongly influenced on symmetric mode amplitude values, thus it was significantly lower. The registered time of arrivals at the AE1 sensor was around 12 μ s and 40 μ s for the S_0 and A_0 modes respectively. In order to decompose the AE signal on extensional and flexural Lamb wave modes, the load was applied in two different configuration as described in detail in previous section. Comparing obtained results, it can be observed that configuration of applied load did not meaningfully influenced on captured acoustic emission signal. Those small differences might be compare by using basic signal parameters. In all cases, elastic waves envelopes were represented by close contours. Similarly, the maximum amplitudes, as well as the rise times were comparable. The main differences could be noticed in signal time duration that varied in dependence of fiber layers configuration. In the point of view of current analysis, the energy of acoustic signal represented by the area under rectified envelope could be the most appropriate parameter to assess the influence of load application method. Nevertheless, in this article, the energies of acoustic signals were compared quantitatively without any advanced calculations. Based on this observations, it could be noticed that the greatest amount of energy were registered for composite plate models with 45° and 60° fiber orientation angles.

In the Table 2 presented values of Lamb wave velocities of separate modes A_0 and S_0 determined numerically in composite plates for different fiber

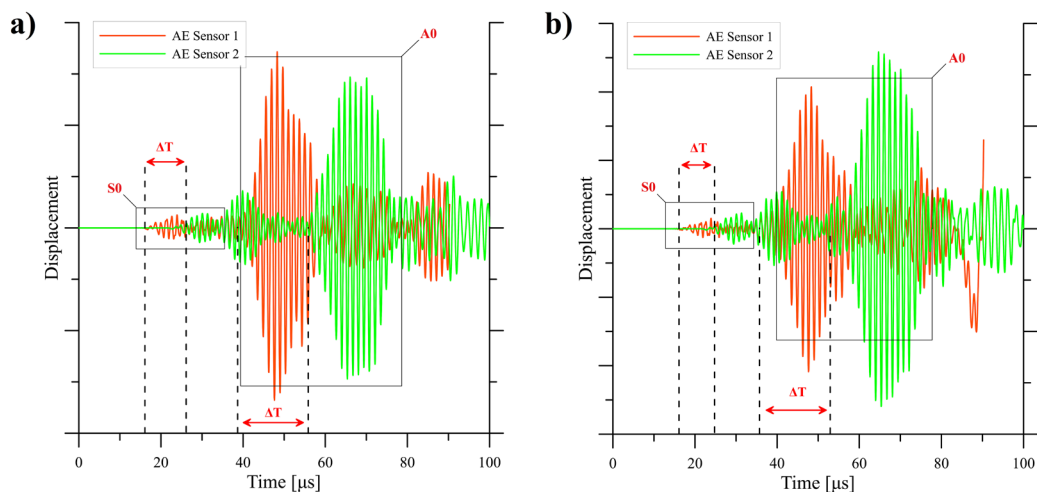


Fig. 2. Normalized displacements versus time registered by two sensors for UD composite plate model: a) for LC-1 configuration b) for LC-2 configuration

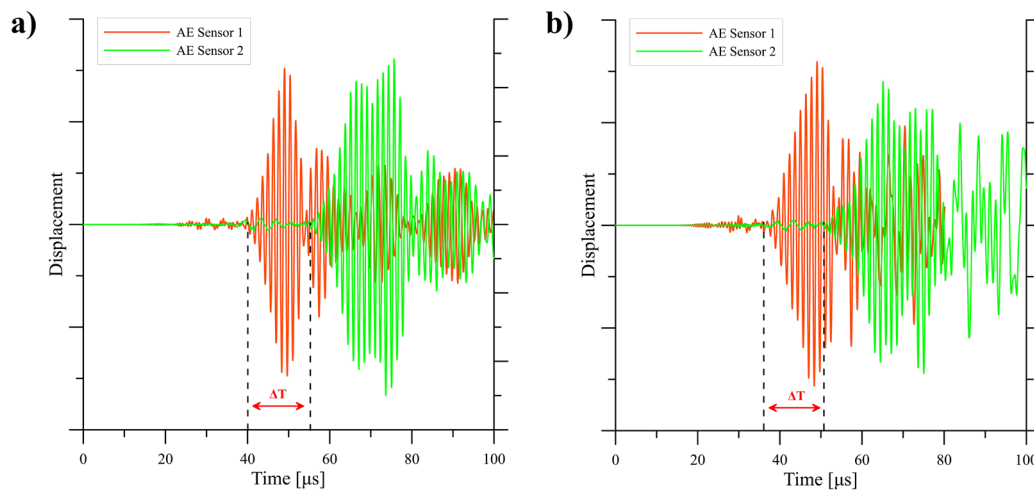


Fig. 3. Normalized displacements versus time registered by two sensors for MD 30 composite plate model: a) for LC-1 configuration b) for LC-2 configuration

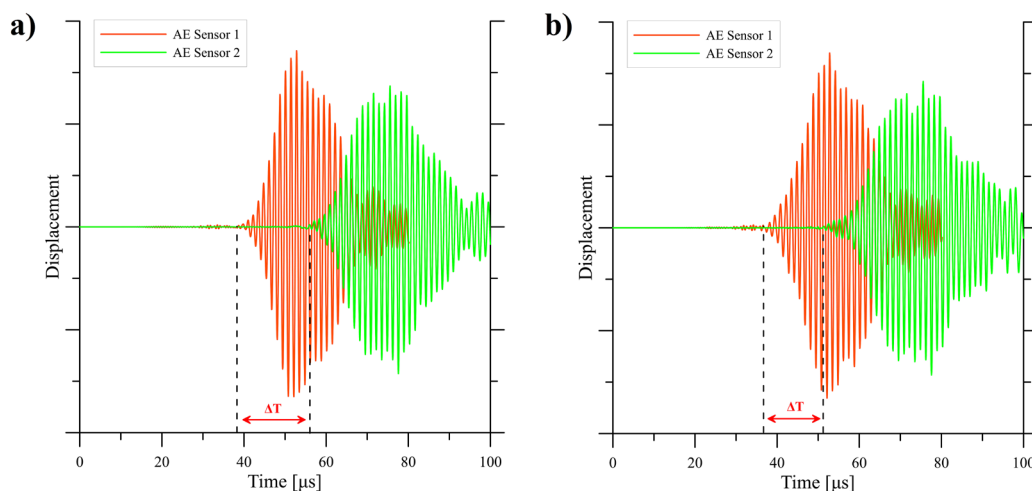


Fig. 4. Normalized displacements versus time registered by two sensors for MD 45 composite plate model: a) for LC-1 configuration b) for LC-2 configuration

orientation angles. All values were calculated by using Equation 5. Differences of arrival times ΔT were taken from numerical data registered by the acoustic sensors AE1 and AE2 modeled at appropriate nodes. The procedure of determination the ΔT values were clearly presented in Figure 2. It can be observed, that in all cases symmetric mode propagated faster than asymmetric mode. For composite plate model with unidirectional fibers orientation along x axis the Lamb waves velocities reached the greatest values equals 5882 m/s and 2994 m/s for S_0 and A_0 modes respectively. With growth of θ angle values of the Lamb waves velocities became smaller reaching minimum for MD-45 laminates – for which the $V_{S_0} = 3378$ m/s and the $V_{A_0} = 2688$ m/s. For composite plate with 60° fiber orientation angles those values were 4970 m/s for the extensional mode and

2874 m/s for the flexural mode. In case of the MD-90 plate, values of the V_{S_0} and the V_{A_0} were equal 3876 m/s and 2747 m/s respectively. Moreover, it is worth to emphasize, that regardless of fiber orientation angles the values of propagation velocities in asymmetric mode were on similar average level 2838 m/s. On the other hand, for the Lamb wave symmetric mode, those values exhibited greater discrepancies. Such significant differences between wave velocities of the S_0 and the A_0 modes were evidenced on the propagation contour plots presented the UD and MD-45 plate models for two different time increments (Figure 7 and 8). First instance regarded to time 3 μ s after the load excitation and the second subplot concerned instance for time $t = 15 \mu$ s. It can be observed, that for all cases, Lamb waves started to propagate in elliptical trajectory and during

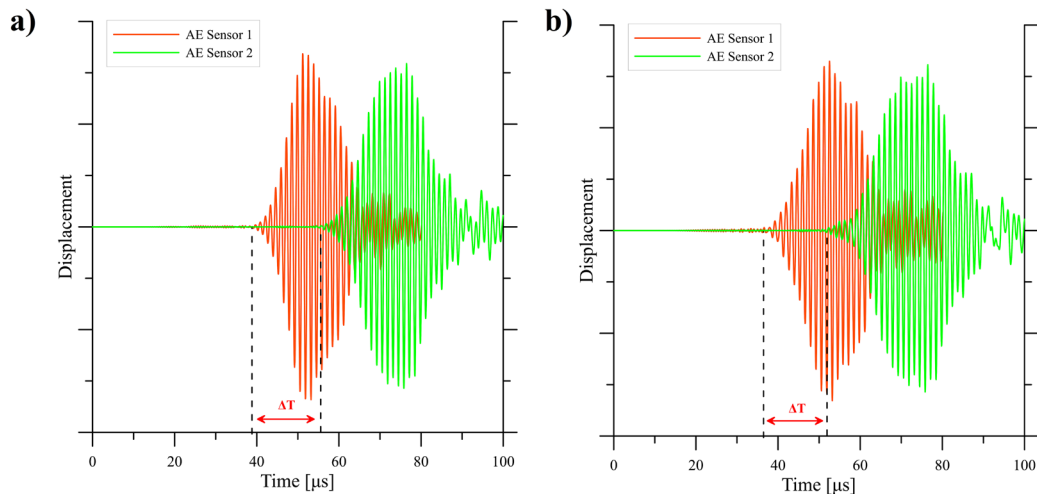


Fig. 5. Normalized displacements versus time registered by two sensors for MD 60 composite plate model: a) for LC-1 configuration b) for LC-2 configuration

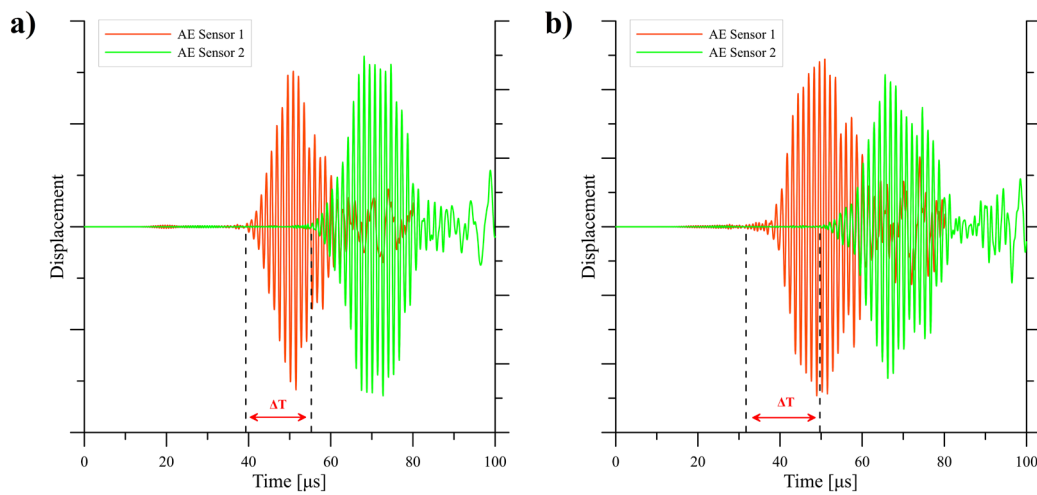


Fig. 6. Normalized displacements versus time registered by two sensors for MD 90 composite plate model: a) for LC-1 configuration b) for LC-2 configuration

subsequent period of time it changed direction according to the fiber orientations in stacking sequences assigned to composite plate model. This effect is well visible for 15 μs time increment. The propagation trajectories of A_0 modes were less extensive, that proved lower values of calculated Lamb wave velocities.

In Figures 9 and 10 presented through-thickness deformations of composite plate with different layers configurations in the XZ plane caused by propagation of the extensional and the flexural modes. It should be highlighted, that for S_0 mode the tensors of deformations along x axis were symmetric while for the A_0 mode it were

Table 2. Lamb wave modes velocities in longitudinal direction obtained for composite plate laminates with different fiber orientation angles

Type of laminates	Lamb wave velocity [m/s]	
	S_0 mode	A_0 mode
UD	5882	2994
MD-30	3817	2890
MD-45	3378	2688
MD-60	4970	2874
MD-90	3876	2747

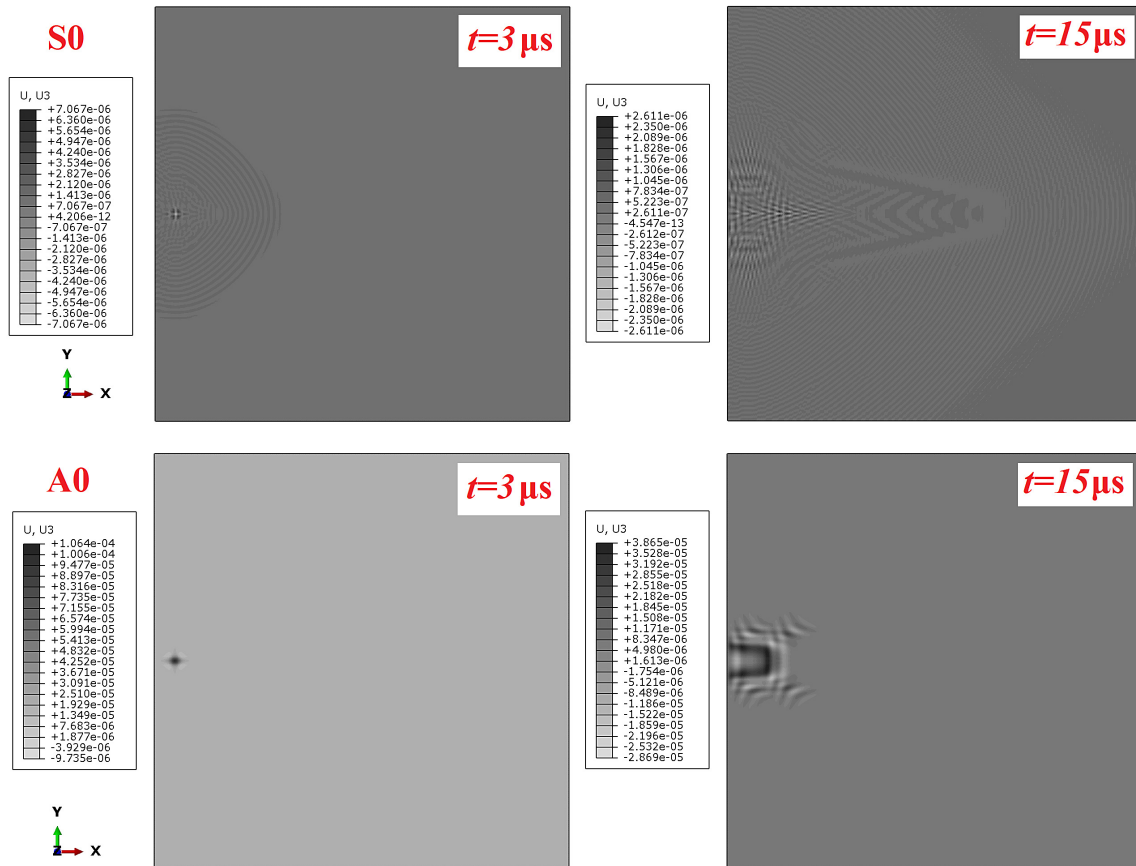


Fig. 7. Contour plot of Lamb wave propagation in UD composite plate

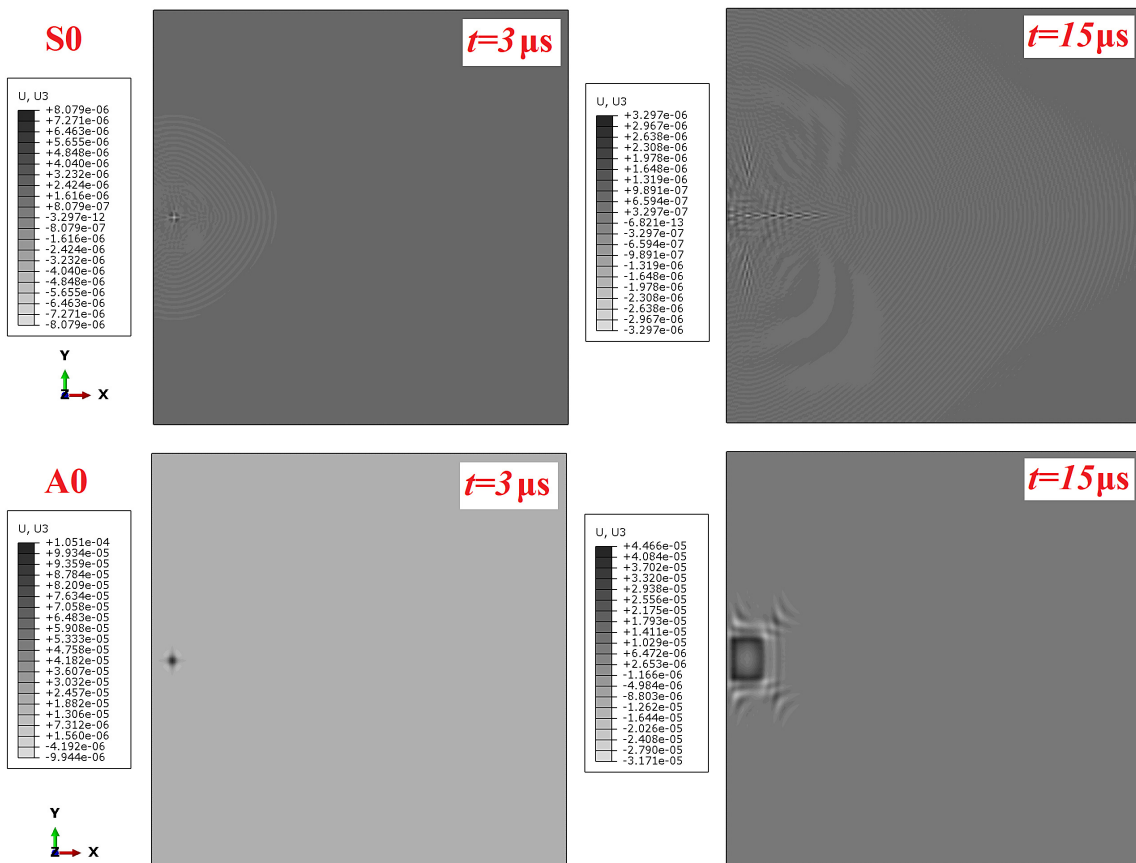


Fig. 8. Contour plot of Lamb wave propagation in MD-45 composite plate

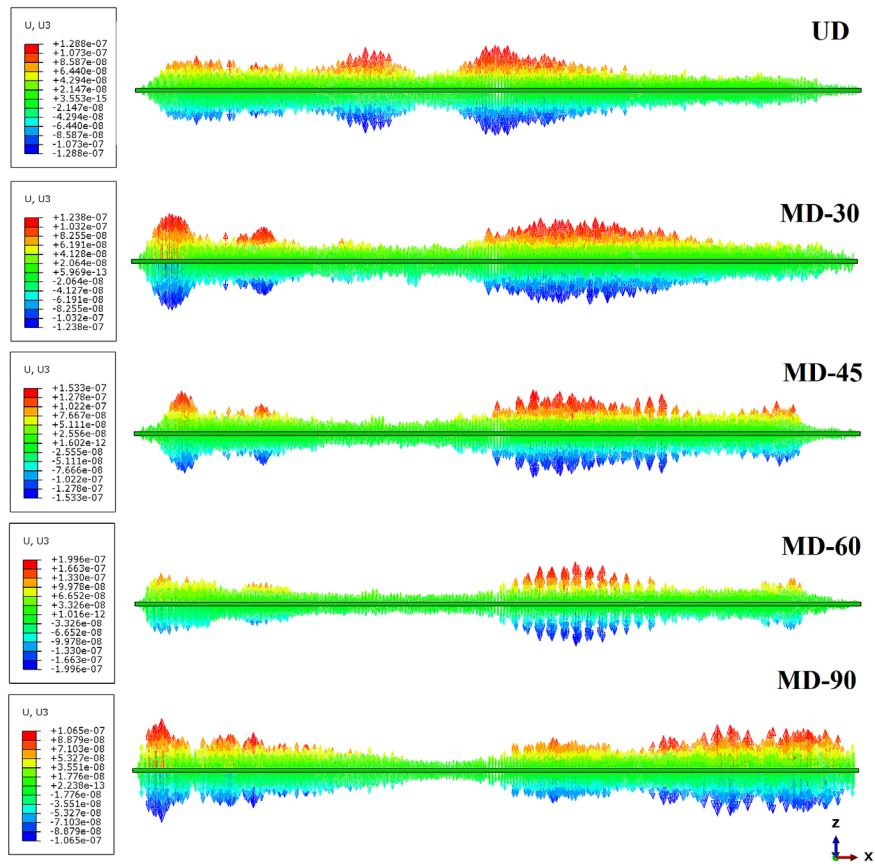


Fig. 9. Through-thickness deformation of composite plate caused by S_0 mode

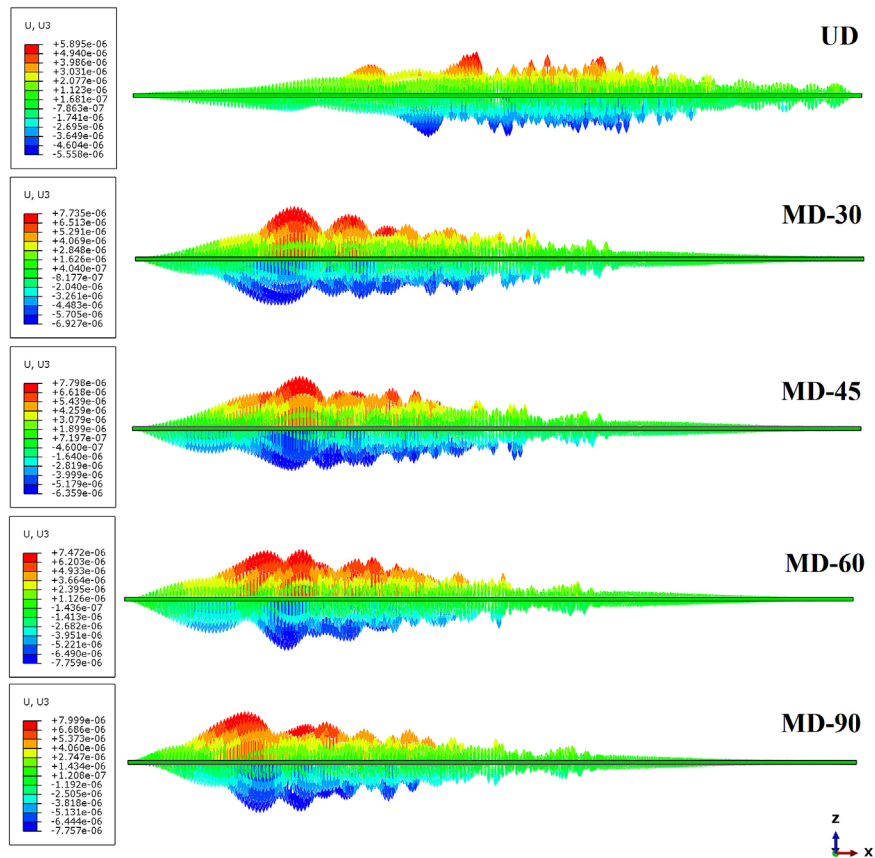


Fig. 10. Through-thickness deformation of composite plate caused by A_0 mode

asymmetric. Presence of this phenomenon confirmed reliability of the finite element numerical simulations. Significant differences in through-thickness deformations can be observed comparing deformation contour plots obtained for plate with unidirectional fiber orientation angle with those obtained for multidirectional stacking sequences. This situation occurred both for the S_0 and A_0 modes. For the unidirectional plate the greater deformation appeared near mid-length of specimen. For the M-30, M-45 and M-60 laminates, deformation caused by the symmetric mode reached maximum values slightly behind of half of the cross-sectional plate model. On the other hand, in case of the asymmetric deformation in the M-30, M-45 and M-60 specimens, the greatest values of displacement in z direction were observed near the node where load was applied. Subsequently, those values gradually decreased reaching zero at the end of the plate. It suggested, that the asymmetric mode was attenuated faster than the extensional S_0 mode. In the point of view of quantitative analysis of Lamb wave propagation in multidirectional composite plates the flexural mode generated slightly greater through-thickness deformations than the symmetric mode. The greatest value of the displacement in z direction equal 7.99×10^{-6} mm was registered for asymmetric M-90 laminate on contrary to the M-90 symmetric plate, for which the value of the displacement U_3 equal 1.06×10^{-7} mm was minimum.

CONCLUSIONS

In this paper presented results of numerical finite element simulations of the Lamb wave propagation in composite plate with different fiber orientation angles. All simulations were conducted in the Abaqus/CAE software by using the dynamic/explicit solver. The numerical model was built with C3D8R brick elements. Refers to the obtained results, the main conclusions can be drawn:

- On contrary to the acoustic emission signal registered during typical experimental AE measurements, numerical FE simulations allowed to decompose the captured Lamb wave on its separate the S_0 and the A_0 modes.
- The greatest values of elastic wave velocities were determined for the symmetric mode reaching maximum for the unidirectional plate model. In composite laminates with multidirectional configuration, due to material

anisotropy, values of the S_0 velocities were lower. In case of the asymmetric mode, the values of V_{A_0} were equal around 2838 m/s.

- Considering the normalized displacement versus time plots and the contour plots of wave propagation, it can be observed that the extensional mode propagated in the material much faster than the flexural mode. It was in convergence with analytically determined Lamb wave velocities. Additionally, the S_0 mode was characterized by the continuous signal whereas the A_0 mode by the burst signal.
- Presented in Figures 9 and 10 the through-thickness deformation of composite plates caused by the effect of propagated Lamb wave proved the reliability of FE simulations. For the S_0 mode, deformation contours were symmetric with respect to the cross section of plate model while for the A_0 those deformations were significantly asymmetric. Analysis of these deformations allowed to recognize the real behavior of Lamb wave modes separately.
- The excitation load configuration had not considerable effects on obtained results, but enabled to decompose the AE signal.

To sum up, the AE measurements can be successfully modeled by using the guided Lamb wave. Appropriate recognition of separate modes behaviors and its velocities is crucial during effective planning and execution of the structural health monitoring of composite structures by using the experimental acoustic emission testing.

Acknowledgements

The grant was financed in the framework of the pro-quality program of Lublin University of Technology „Grants for grants” 2/GnG/2023.

REFERENCES

1. Mueller I, Memmolo V, Tschöke K, Moix-Bonet M, Möllenhoff K, Golub M, et al. Performance Assessment for a Guided Wave-Based SHM System Applied to a Stiffened Composite Structure. *Sensors* (Basel). 2022;22(19).
2. Xu B, Wu J, Wang M. Study of modal acoustic emission to monitor the impact damage in a composite plate. *J. vibroeng.* 2017;19(5):3335–48.
3. Šofer M, Šofer P, Pagáč M, Volodarskaja A, Babiuch M, Gruň F. Acoustic Emission Signal Characterisation of Failure Mechanisms in CFRP Composites

- Using Dual-Sensor Approach and Spectral Clustering Technique. *Polymers (Basel)*. 2022;15(1).
4. Li W, Liu Y, Jiang P, Guo F, Cheng J. Study on Delamination Damage of CFRP Laminates Based on Acoustic Emission and Micro Visualization. *Materials (Basel)*. 2022;15(4).
 5. Holford KM, Pullin R, Evans SL, Eaton MJ, Hensman J, Worden K. Acoustic emission for monitoring aircraft structures. *Proceedings of the Institution of Mechanical Engineers, Part G: Journal of Aerospace Engineering*. 2009;223(5):525–32.
 6. Su Z, Ye L, Lu Y. Guided Lamb waves for identification of damage in composite structures: A review. *Journal of Sound and Vibration*. 2006; 295(3-5):753–80.
 7. Rzeczkowski J, Samborski S, Moura M de. Experimental Investigation of Delamination in Composite Continuous Fiber-Reinforced Plastic Laminates with Elastic Couplings. *Materials (Basel)*. 2020;13(22).
 8. Rzeczkowski J, Samborski S. Experimental and Numerical Research of Delamination Process in CFRP Laminates with Bending-Twisting Elastic Couplings. *Materials (Basel)*. 2022;15(21).
 9. Czarnocki P. Resistance of Polymeric Laminates Reinforced with Fabrics against the Growth of Delaminations. *Materials (Basel)*. 2021;14(23).
 10. Sadler J, Maev RG. Experimental and theoretical basis of Lamb waves and their applications in material sciences. *Can. J. Phys.* 2007;85(7):707–31.
 11. Yang C, Ye L, Su Z, Bannister M. Some aspects of numerical simulation for Lamb wave propagation in composite laminates. *Composite Structures*. 2006;75(1-4):267–75.
 12. Barroso-Romero M, Gagar D, Pant S, Martinez M. Wave Mode Identification of Acoustic Emission Signals Using Phase Analysis. *Acoustics*. 2019;1(2):450–72.
 13. Hameed MS, Li Z, Chen J, Qi J. Lamb-Wave-Based Multistage Damage Detection Method Using an Active PZT Sensor Network for Large Structures. *Sensors (Basel)*. 2019;19(9).
 14. Milosavljevic D, Zmindak M, Dekys V, Radakovic A, Cukanovic D. Approximate phase speed of Lamb waves in a composite plate reinforced with strong fibres. *J Eng Math*. 2021;129(1):3.
 15. Cheng L, Xin H, Groves RM, Veljkovic M. Acoustic emission source location using Lamb wave propagation simulation and artificial neural network for I-shaped steel girder. *Construction and Building Materials*. 2021;273(1):121706.
 16. Barski M, Pająk P. Determination of Dispersion Curves for Composite Materials with the Use of Stiffness Matrix Method. *Acta Mechanica et Automatica*. 2017;11(2):121–8.
 17. Luca A de, Sharif-Khodaei Z, Aliabadi MH, Caputo F. Numerical Simulation of the Lamb Wave Propagation in Impacted CFRP Laminate. *Procedia Engineering*. 2016;167:109–15.
 18. Tumšys O. Experimental Method for Simultaneous Determination of the Lamb Wave A0 Modes Group and Phase Velocities. *Materials (Basel)*. 2022;15(9).
 19. Ono K. Experimental Determination of Lamb-Wave Attenuation Coefficients. *Applied Sciences*. 2022;12(13):6735.
 20. Shpak AN, Mueller I, Golub MV, Fritzen CP. Theoretical and experimental investigation of Lamb waves excited by partially debonded rectangular piezoelectric transducers. *Smart Mater. Struct.* 2020;29(4):45043.
 21. Habibi M, Laperrière L. Combining Digital Image Correlation and Acoustic Emission to Characterize the Flexural Behavior of Flax Biocomposites; 2023.
 22. Hosseini SMH, Kharaghani A, Kirsch C, Gabbert U. Numerical simulation of Lamb wave propagation in metallic foam sandwich structures: A parametric study. *Composite Structures*. 2013;97(10):387–400.